

Thermophysical Properties of Pharmaceutically Compatible Buffers at Sub-Zero Temperatures: Implications for Freeze-Drying

Evgenyi Y. Shalaev^{1,4}, Tiffany D. Johnson-Elton^{1,2}, Liuquan Chang³, and Michael J. Pikal³

Received October 10, 2001; accepted November 1, 2001

Purpose. To evaluate crystallization behavior and collapse temperature (T_g') of buffers in the frozen state, in view of its importance in the development of lyophilized formulations.

Methods. Sodium tartrate, sodium malate, potassium citrate, and sodium citrate buffers were prepared with a pH range within their individual buffering capacities. Crystallization and the T_g' were detected during heating of the frozen solutions using standard DSC and modulated DSC.

Results. Citrate and malate did not exhibit crystallization, while succinate and tartrate crystallized during heating of the frozen solutions. The citrate buffer had a higher T_g' than malate and tartrate buffers at the same pH. T_g' vs. pH graphs for citrate and malate buffers studied had a similar shape, with a maximum in T_g' at pH ranging from 3 to 4. The T_g' maximum was explained as a result of a competition between two opposing trends: an increase in the viscosity of the amorphous phase because of an increase in electrostatic interaction, and a decrease in the T_g' because of an increase in a water concentration of the freeze-concentrated solution.

Conclusion. Citrate buffer was identified as the preferred buffer for lyophilized pharmaceuticals because of its higher T_g' and a lower crystallization tendency.

KEY WORDS: lyophilization; freezing; buffers; collapse; glass transition; DSC.

INTRODUCTION

Many pharmaceuticals contain a buffer to control pH, to ensure optimal chemical and physical stability of a drug molecule. Buffering capacity and a possibility of a buffer-specific catalysis are the major buffer properties which are usually taken into consideration in development of liquid pharmaceutical formulations (1). For lyophilized formulations, there are two additional physical chemical parameters to consider, i.e., buffer crystallization potential at sub-ambient temperatures, and the collapse temperature. A buffer component may crystallize during freezing producing significant pH changes (2) that are usually undesirable and should be avoided. Crystallization and pH changes of phosphate buffer at sub-zero temperatures were studied in detail in the presence of different metal ions and in a wide range of pH and concentration (3–7). Systematic studies of equilibrium freezing behavior of

phosphate buffer were performed by van den Berg *et al.* in 1950–1960. In these studies, liquid (unfrozen) portions of a frozen solution was physically separated at sub-zero temperatures, and the pH and composition of the liquid portion were measured at room temperature (2–4). Later, other methods were used such as measurements of pH at sub-zero temperatures with a low-temperature electrode (5,6,8,9) and pH indicators (10), X-ray diffraction measurements at sub-ambient temperatures (7), and DSC studies (11–13). Significant pH changes were observed depending on a metal ion type and experiment setup (sample size, cooling rate). Based on these results, phosphate buffer is generally regarded to be undesirable for lyophilized formulations, at least if high buffer concentrations are required to maintain high buffer capacity (14). There are some studies of other buffers of pharmaceutical interest (citrate, glycine, succinate, carbonate) in very narrow ranges of solution pH and concentration (9,10,15).

Another physical chemical parameter critical for lyophilization is the collapse temperature (16). Freeze drying above the collapse temperature produces loss of the cake-like structure that one desires. Obviously, materials with a higher collapse temperature can be freeze-dried at a higher temperature, hence providing a faster and more robust lyophilization cycle. If the collapse temperature of a formulation is relatively low, it is more difficult and sometimes impossible to lyophilize such a formulation in a practical process. As a rule, presence of amorphous buffer in a formulation decreases the collapse temperature resulting in recommendations to minimize buffer concentration in lyophilized formulations (17). The collapse temperature can be measured by different techniques, with freeze drying microscopy and DSC being the methods of choice in most cases. With DSC, a thermal transition denoted T_g' is measured as the temperature of an endothermic step which precedes the melting endotherm on DSC heating curves of frozen solutions (16). It should be stressed that interpretation of the physical nature of the T_g' thermal event is still controversial. There are two alternative interpretation of the T_g' . The T_g' thermal event has been explained as either a glass transition of the freeze-concentrated solution (18,19), or onset of ice melting marked as T_s (softening temperature) (20), or T_m (21). Despite of this controversy, there is a common agreement that the T_g' corresponds closely to the collapse temperature, the collapse temperature normally being higher by 1–3°C (16). Frequently, one detects a second very weak apparent glass transition roughly 20°C lower than T_g' . This lower transition is denoted T_g'' , and does not appear to be related to the collapse phenomena. The T_g' of several acids and bases (ascorbic acid, citric acid, glycine, HEPES, TRIS) and buffers (citrate, TRIS, acetate, glycine, and histidine) has been determined in (12,15,22–25). In majority of these studies, the T_g' was determined at a single pH value (with exceptions (25) for histidine and (15) for glycine). There is a lack of systematic data on collapse temperatures and crystallization behavior as a function of pH for buffers of pharmaceutical significance.

In the present study, crystallization behavior and collapse temperature of several buffers (citrate, succinate, malate, tartrate) have been studied using DSC. Each buffer was prepared at different pH to cover the buffering range of the particular buffer. It should be emphasized that variation of

¹ Groton Laboratories, Pfizer Inc., Groton, Connecticut 06340.

² School of Pharmacy, University of Minnesota, Minnesota.

³ School of Pharmacy, University of Connecticut, Storrs, Connecticut 06269.

⁴ To whom correspondence should be addressed. (e-mail: evgenyi_y_shalaev@groton.pfizer.com)

pH is equivalent to variation of the molecular/ionic species in solution as pH variations alters the extent of ionization of buffer. Significant changes in the crystallization behavior, and the T_g ' were observed as a function of solution pH. An unexpected pattern of T_g ' changes with solution pH was observed for all buffers studied with T_g ' having a maximum around pH 4. In addition, it appeared that a metal ion type (i.e., Na vs. K) has a significant impact on T_g ' of a citrate buffer.

MATERIALS AND METHODS.

Materials

Reagent grade succinic acid and DL-malic acid were purchased from Fisher Scientific and Sigma, respectively. Citric acid of USP grade, L-(+)-tartaric acid of NF grade, and sodium hydroxide of NF grade were obtained from JT Baker. In addition, DL-tartaric acid of reagent grade from EM Science was used. Deionized water was used to prepare all of the buffer solutions that were studied. Citric acid, succinic acid, tartaric acid, malic acid were prepared as 0.25M solutions. The acids were titrated with 0.25M sodium hydroxide to the desired buffer pH. In addition, citric acid/potassium hydroxide solutions were prepared by the same methods. Weight of the added base was measured. The pH range studied was chosen as to be within the pH range where the buffer system had significant buffering capacity (1).

DSC Experiments

DSC experiments were performed with a Perkin-Elmer Pyris 1 instrument and TA Instruments modulated DSC 2920 instrument equipped with Refrigerated Cooling System. Approx. 15 μ l of solution were placed in aluminum pans, and empty aluminum pans were used as a reference with both instruments. Other details of the experiments performed with the Perkin-Elmer instrument are as follows. The instrument was calibrated using melting points of indium at heating rate 10°C/min. The calibration was checked using de-ionized water. The uncertainty in the temperature calibration was estimated to be within 1.5°C. Samples were cooled to -60°C at 10°C/min, then held at -60°C for 5 min, and then heated from -60°C to 25°C at 10°C/min. The T_g ' and T_g '' temperatures were determined as extrapolated onset temperatures using Pyris software. Experiments were performed with the TA instrument as follows. Calibrations were performed using indium as standard at a heating rate 10°C/min and 1°C/min for standard and modulated method, respectively. The purge gas used was nitrogen with a flow rate at 50 ml/min. Samples were run in two different modes: (i) Standard DSC mode, which the samples were cooled to -60°C at 10°C/min, equilibrate at -60°C for 5 min, and then heated to 25°C at 10°C/min. (ii) Modulated DSC mode, which the samples were cooled to -60°C and then heated to 25°C at the same heating and cooling rate of 1°C/min. The run was modulated with an amplitude $\pm 0.5^\circ\text{C}$ and a period 100 seconds. The T_g ' and T_g '' temperatures were determined as extrapolated onset temperatures using TA universal analysis software.

RESULTS

Typical DSC curves of sodium and potassium citrate buffer are shown in Figs. 1a and 1b, respectively (ice melting

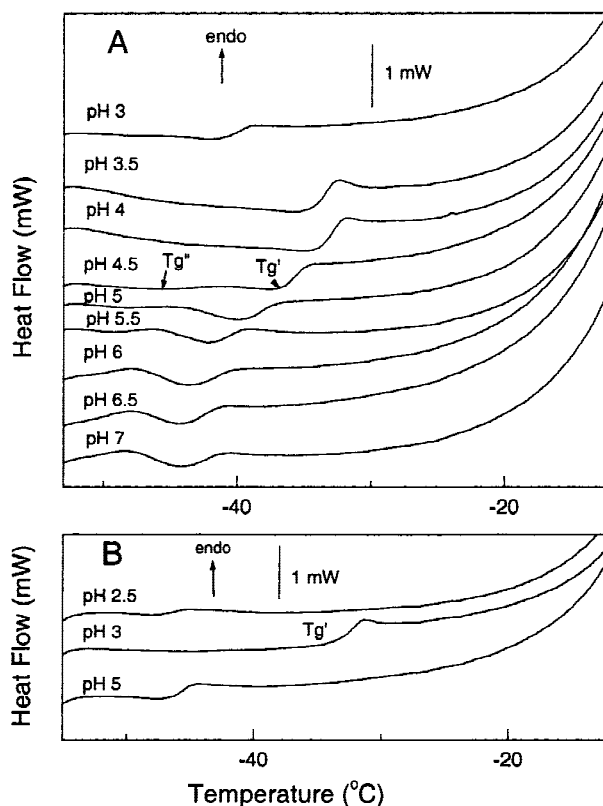


Fig. 1. Representative DSC heating curves of citric acid/NaOH (A) and citric acid/KOH (B) solutions. Magnified low-temperature portions of the DSC scans are shown. Numbers present solution pH. Scanning rates: 10°C/min. The experiments were run with Perkin-Elmer Pyris-1 DSC.

endotherm is not shown). Two consecutive endothermic events, T_g '' and T_g ', were observed in majority of cases which is typical for frozen aqueous solutions (18–21). There is a common agreement that a higher temperature event (T_g ') corresponds to the collapse temperature.

A "dip" in the baseline was observed on DSC heating curves of sodium citrate at pH's from 5 to 7. Such "dip" on a DSC heating curve could be due to an exothermic event such as crystallization; if this is the case, assignment of the T_g ' event is uncertain. To determine if crystallization occurred in these samples, two types of DSC experiments were performed. In the first experiment, a thermal cycling study was performed; thermal cycling allows one to separate reversible thermal transitions (such as glass transition and melting) from irreversible transitions (such as crystallization) and artifacts (such an event associated with a change in a sample shape in the DSC pan) (20,26). In this thermal cycling experiment, the frozen solution was first heated to -44.5°C (which is the onset temperature of the thermal event under consideration) followed by cooling to -65°C, and then heated from -65 to 25°C. If the thermal event under consideration is the (ice) crystallization exotherm, the second DSC heating curve should have a different appearance because crystallization would occur only during the first run and thus would be irreversible. In particular, the temperature of the first endothermic step would be shifted to higher temperature (if ice crystallize) or to the lower temperature (if solute crystallizes). Results of the thermal cycling experiment are shown in Fig.2a. It can be seen

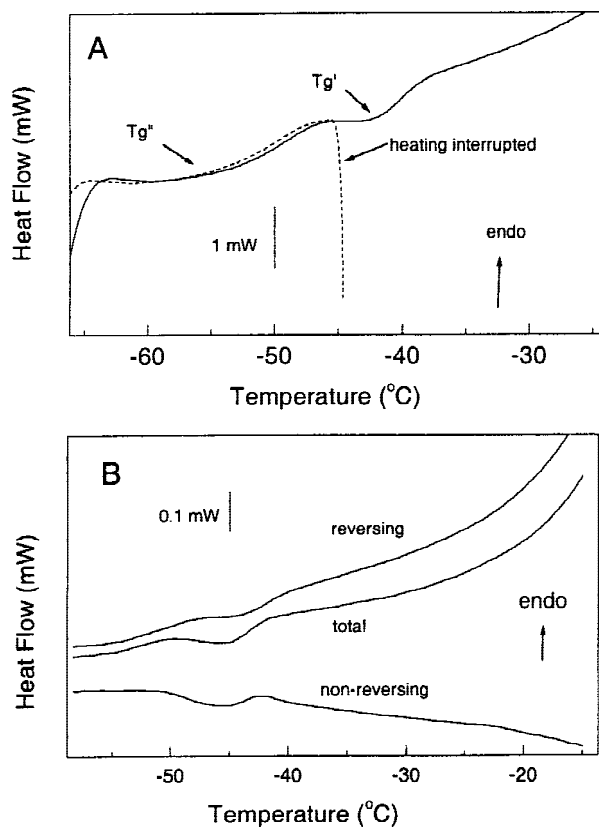


Fig. 2. Thermal cycling (A) and modulated DSC (B) runs of citric acid/NaOH solution with pH 6. The data were obtained with TA DSC.

that first and second heating curves are practically identical, i.e., the position of the first endothermic step did not change on the second scan. Hence, the results of the thermal cycling experiment suggested that crystallization did not occur during heating of the sodium citrate buffer solution.

In addition, modulated DSC experiments were performed. Modulated DSC allows separation of irreversible (such as crystallization) and reversible (such as glass transition) thermal events (19). Modulated DSC heating curves are shown in Fig. 2b. The reversing heat flow curve shows two consecutive endothermic events (T_g'' and T_g'), similar to a regular DSC scan. The nonreversing heat flow curve shows that there is perhaps some crystallization, as evident from the weak exothermic peak centered at -45°C ; however the magnitude of the exotherm is very small, and the modulated DSC data are not consistent with a significant amount of crystallization occurring during heating the frozen solution. T_g' temperature determined from the modulated DSC run is slightly lower than determined from the regular DSC scan; however, the difference is close to the estimated experimental error. Both thermal cycling and modulated DSC experiments indicate that regular (non-modulated) DSC scans can be used to measure T_g' and T_g'' of the sodium citrate solutions at pH 5 to 7. We did not attempt to investigate the origin of the apparent "dip" which was observed prior to the T_g' event for sodium citrate solutions at pH 5 to 7 in more detail. Figure 3 shows T_g' and T_g'' as a function of pH for sodium citrate and potassium citrate. There is good agreement between results obtained with the two different DSC instruments and with

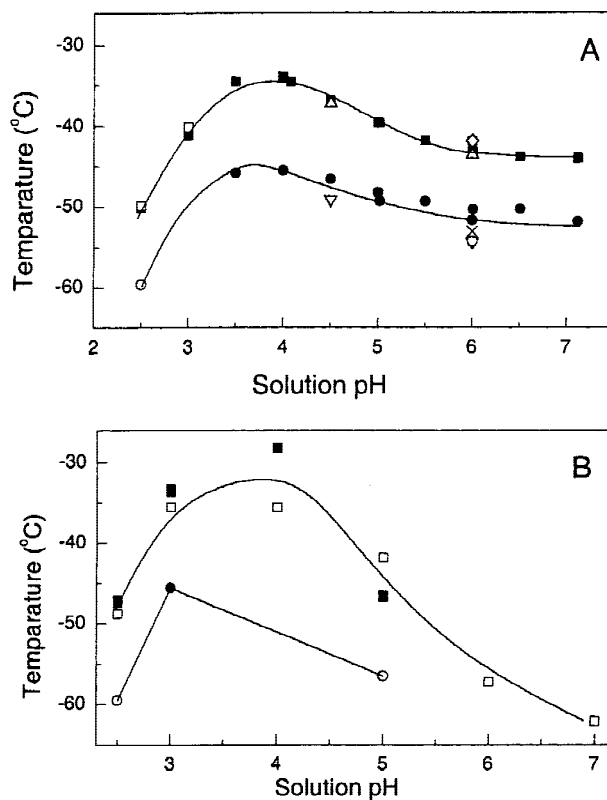


Fig. 3. T_g' and T_g'' of citric acid/NaOH (A) and citric acid/KOH (B) solutions as a function of pH. \square : T_g' measured with TA DSC; \blacksquare : T_g' measured with Perkin-Elmer DSC; \square : T_g'' measured with TA DSC; \bullet : T_g'' measured with Perkin-Elmer DSC; \triangle : T_g' measured with TA MDSC; ∇ : T_g'' measured with TA DSC; \diamond : T_g' measured with TA DSC in thermal cycling experiment; \times : T_g'' measured with TA DSC in thermal cycling experiment. Each data point corresponds to a single DSC run. Lines are given as a visual aid.

different sample preparations. For sodium citrate, both T_g' and T_g'' passed through a maximum at pH ~ 4 . Similarly, for potassium citrate, T_g' passed through maximum between pH 3 and 4.

DSC curves of malic acid/NaOH solutions had a similar appearance to the citrate buffer solutions with one or two endothermic steps (T_g'' and T_g') followed by ice melting peak (curves are not shown). T_g'' and T_g' of malate buffer as a function of solution pH are shown in Fig. 4a. Again, T_g' goes through a maximum at pH 4.

Succinic acid/NaOH and tartaric acid/NaOH solutions demonstrated a different thermal behavior. Representative DSC heating curves of succinic acid/NaOH and tartaric acid/NaOH systems are shown in Figs. 5 and 6, respectively. Buffer crystallization occurred in all three succinic acid/NaOH mixtures studied (pH 4, 5, 6) as evidenced from observation of both the exothermic peak (D) and endothermic peaks (M) prior to ice melting. A weak endothermic step immediately before the crystallization exotherm, which was observed at pH 5 and 6 in succinate buffer (Fig. 5, inset), may be assigned to either T_g' or T_g'' . We did not attempt to characterize this transition in more detail. Crystallization was not detected in pure succinic acid. Lack of crystallization observed for the free acid indicates that a salt (not the free acid) crystallized during heating of frozen succinic acid/NaOH solutions. In

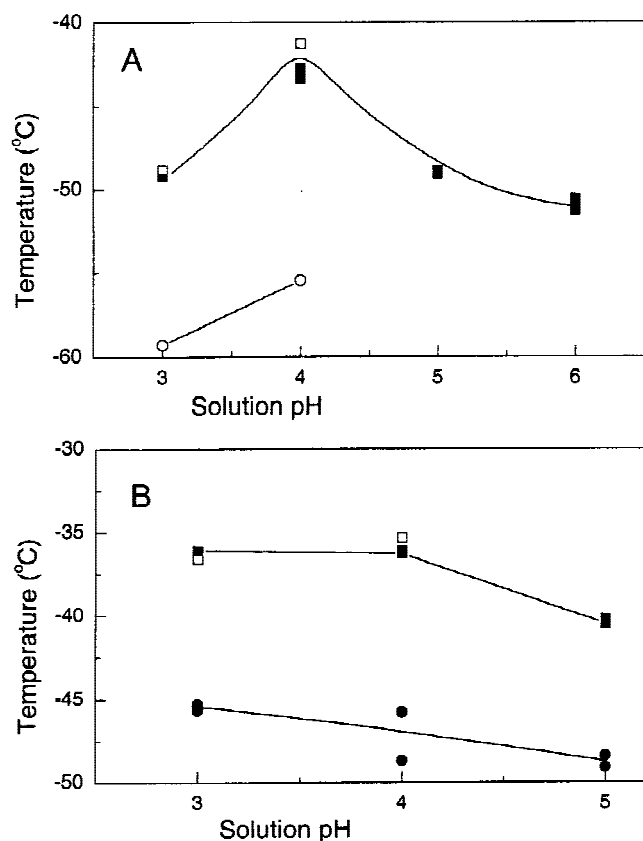


Fig. 4. T_g' and T_g'' of malic acid/NaOH (A) and tartaric acid/NaOH (B) solutions as a function of pH. All data point but open squares in Fig. 4B correspond to solutions prepared with L-(+)-tartaric acid, and open squares correspond to solutions prepared with DL-tartaric acid. See Fig. 3 for other symbols. Each data point corresponds to a single DSC run. Lines are given as a visual aid.

agreement with this hypothesis, both crystallization exotherms and melting endotherms were stronger in succinate solution with pH 6 (solution with a higher salt content). In addition, multiple melting peaks were observed at pH 4 and 5, indicating that several crystalline succinate salts were formed (i.e., perhaps mono- and di-sodium succinate and their hydrates).

A T_g' event followed by a strong crystallization peak was observed in a solution of L-(+)-tartaric acid/NaOH at pH 3 (Fig. 6a). In addition, a weaker exotherm was observed in solution of pH 4. We note that a solution of DL-tartaric acid/NaOH at pH 3 had a much weaker exothermic event (scan is not shown) indicating that the racemic reagent had a lower crystallization tendency. Fig. 4b shows T_g' and T_g'' vs. pH for tartaric acid/NaOH system. Despite of the difference in crystallization behavior, there was no significant difference in the T_g' between solutions prepared with either L-(+)-tartaric acid or DL-tartaric acid. Both T_g' and T_g'' for tartaric acid/NaOH solutions were slightly higher at more acidic pH (pH 3) than at pH 5.

DISCUSSION

T_g' vs. pH profiles with a maximum were observed for citrate and malate buffers. Such behavior has not been reported in the literature. The lack of literature precedent is not

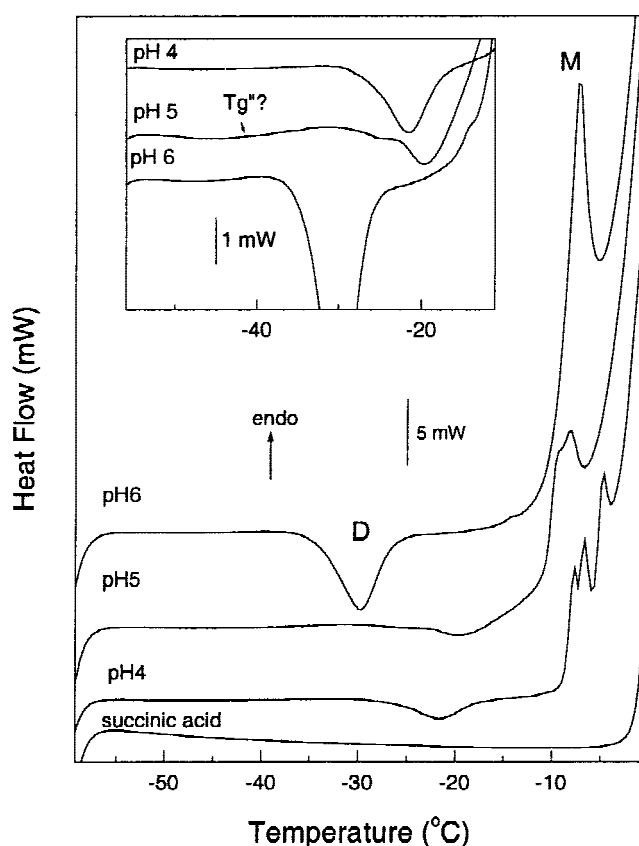


Fig. 5. Representative DSC heating curves of succinic acid/NaOH solutions. Inset shows magnified portions of DSC curves with a non-identified thermal event (which may be either T_g' or T_g''). Scanning rates: $10^\circ\text{C}/\text{min}$.

surprising. Indeed, there is only one systematic study of T_g' vs. pH described in the literature (25). It was observed that T_g' of frozen histidine solutions decreased with an increase in pH (25). Such a decrease in T_g' was explained as due to increased salt concentration.

In this work, an opposite trend in T_g' vs. pH was observed, i.e., T_g' first increased with increasing salt concentration. To illustrate this point, T_g' is presented as a function of NaOH/citric acid mole ratio (Fig. 7). An increase in sodium content initially produced a significant increase in T_g' (which is opposite to the trend reported in (25) for histidine), followed by a gradual decrease in T_g' with further increase in sodium content.

An increase in T_g' with increasing sodium content can be rationalized in terms of increasing ionic interactions as the concentration of ionic species increases. Indeed, salts frequently have higher glass transition temperatures than the corresponding free acids. For the organic acid, indomethacin, T_g of the free acid was $\sim 75^\circ\text{C}$ lower than that of the sodium salt (27). Hence, the initial increase in T_g' in citrate and malate buffers when pH increased from 2.5 to 4 can be explained on the same basis. That is, ionization allows electrostatic interactions between species and corresponding higher viscosity. However, this "electrostatic interaction" concept alone cannot account for the maximum of T_g' vs. pH. Clearly another effect must be important. Note that, in a freeze-concentrated solution, viscosity (and T_g') depends not only

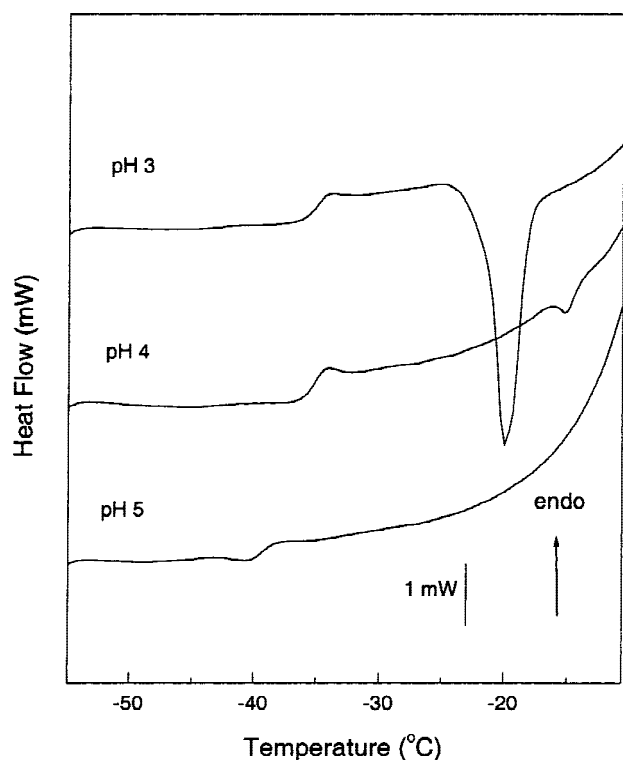


Fig. 6. Representative DSC heating curves of L-(+)-tartaric acid/NaOH solutions. Scanning rates: 10°C/min.

on solutes present (e.g., on salt amount) but also depend strongly on the water content in the unfrozen fraction. We suggest that as pH and salt content in a solution increases further, water content in the freeze-concentrated solution increases to a point where the plasticizing effect of water ultimately results in a decrease in T_g' . Indeed, an increase in the unfrozen water content with salt concentration was reported for sucrose/NaCl solutions (17). The above considerations suggest that, at pH ~4 (i.e., at pH where T_g' maximum is observed) there is a balance between increase in T_g' because of the electrostatic interaction effect, and decrease in T_g' because of the plasticization effect of unfrozen water in the freeze-concentrated solution. The observed difference in behavior of sodium and potassium buffers support the suggestion that a decrease in T_g' is due to an increase in water content in freeze-concentrated solution and not due to a different degree of ionization. Indeed, if this were an extent of ionization effect, a constant difference in T_g' between sodium citrate and potassium citrate would be expected because the state of ionization is independent of the metal ion species present. Different patterns for T_g' of sodium citrate and potassium citrate provides indirect support for the "unfrozen water" explanation. The bigger impact of pH on T_g' for potassium citrate buffer at pH > 5 (i.e., the significant drop in T_g') is consistent with this interpretation. That is, more water remains unfrozen with potassium than with sodium ion. To verify this interpretation, water contents in freeze-concentrated solutions would need to be determined. Alternately, one could measure glass transition temperatures of anhydrous salts as a function of sodium or potassium content. An observed monotonic change of T_g with salt content would lend support to the interpretation.

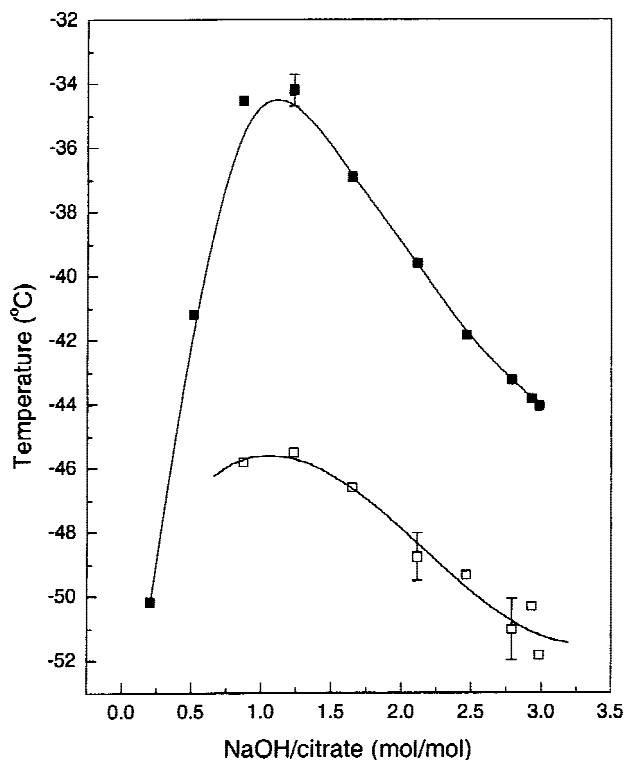


Fig. 7. T_g' and T_g'' of citric acid/NaOH solutions as a function of NaOH/citric acid mole ratio. ■: T_g' ; □: T_g'' . Error bars represent standard deviations. Lines are given as a visual aid.

Crystallization results obtained in the present study agree with a study of pH changes during freezing reported in the literature (10). Here, pH changes during freezing in a number of buffers were evaluated using pH indicators. In particular, succinic acid/NaOH solution at pH 5, and citrate acid/sodium citrate solution at pH 5.5 (i.e., solution pH values before freezing) were studied. In agreement with the DSC results reported here, pH in the citric buffer did not change during freezing which agrees with the lack of crystallization observed in the present DSC study. For succinate buffer, DSC results obtained in this work indicate that succinate crystallized but only during heating of the frozen solutions. Hence, we expect that, during freezing, succinate buffer does not crystallize and significant pH changes during freezing are not expected, which agrees with (10) where pH changes for succinate buffer were not observed during freezing.

Practical Consideration: Implications for Freeze-Drying

One of the most important physical chemical parameters of a material from a freeze-drying perspective is the collapse temperature. It was demonstrated that collapse temperature as measured using freeze-drying microscope was very close to T_g' as determined by DSC (within 1-3°C) (16). Materials which have higher T_g' can be freeze-dried at a higher temperature during primary drying, hence providing a faster and more robust lyophilization cycle. As a rule, pharmaceutical formulations contain several components (drug itself, buffer, bulking agent, stabilizer, preservative, etc.). The T_g' of a mixture depends on T_g' and weight fractions of individual components with an expectation that individual components

which have higher T_g' provide a higher T_g' for the mixture (28).

T_g' as a function of pH for the buffers studied is given in Fig. 8. Citrate buffer has the highest T_g' over the pH range studied. Potassium citrate buffer has the highest T_g' at pH from 2.5 to 4.5 whereas sodium citrate has the highest T_g' at pH 4 to 7. Hence, if consider T_g' alone, sodium citrate would be the preferred choice at pH 2.5 to 4.5, and potassium citrate would be the choice in the pH range of 4.5 to 7.

Another consideration in a buffer choice is its tendency to crystallize in the frozen state. Buffer crystallization is an undesirable process because it causes significant pH changes (several pH units). In particular, relatively high crystallization potential of a phosphate buffer is a reason why it is not usually recommended for use in freeze-dried formulations (14). In this study, we observed crystallization of succinate and tartrate buffers, whereas malate and citrate did not crystallize under the conditions of DSC experiment. Hence, citrate and malate buffers would be the choice from the perspective of crystallization potential.

It should be stressed that the lack of crystallization observed during the DSC experiment does not necessarily mean that citrate and malate will not crystallize during an actual freeze-drying run. Crystallization behavior depends on sample size, cooling rates, and both concentration and type of nucleation centers, the latter being very hard to control. Indeed, it has been shown for phosphate buffer that sample size has a large impact on crystallization tendency (5). Solutions that did not crystallize during DSC experiments did crystallize

during low-temperature powder X-ray diffraction and pH studies where a larger sample volume was used (5). In addition, cooling rates during freeze-drying are usually much lower than the $10^\circ\text{C}/\text{min}$ which was used in our DSC experiments. Lower cooling rates favor crystallization. Hence, any quantitative prediction of crystallization behavior for a particular buffer (or other excipients) during freeze-drying should be treated with some skepticism. However, DSC data can be used to provide qualitative comparisons between different buffers.

Citrate would appear to be the buffer of choice for lyophilized formulations because it has a lower crystallization potential and a higher collapse temperature. It should be stressed, however, that, in addition to the specific lyophilization parameters considered here (i.e., collapse temperature and crystallization potential), other factors such as specific buffer catalysis and buffering capacity, should be considered when finalizing the choice of buffer (1). Moreover, we do not suggest that buffers with a relatively low collapse temperature and relatively high crystallization potential (i.e., succinate buffer) cannot be used in lyophilized formulations. Both collapse temperature and crystallization ability can be modified using other excipients. In particular, if a formulation contains significant amount of an (amorphous) bulking agent or drug itself, collapse temperature can be increased significantly, and buffer crystallization may be suppressed (29). The amount of an amorphous component required to suppress crystallization or to provide for an acceptable T_g' , however, would be lower in case of a buffer with a higher T_g' or with a lower crystallization potential.

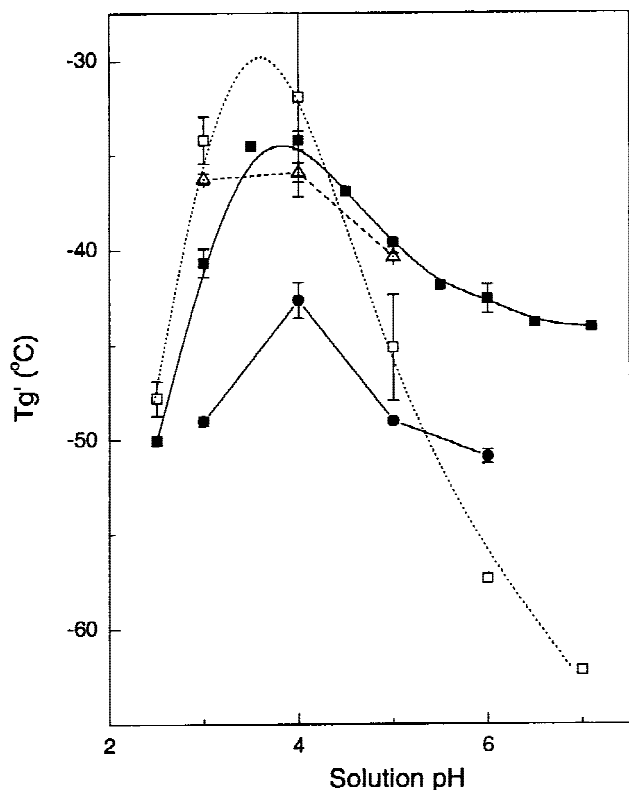


Fig. 8. Summary of collapse temperature (T_g') as a function of pH for buffers studied in this work. ■: sodium citrate; □: potassium citrate; ●: sodium malate; △: sodium tartrate. Error bars represent standard deviation. Lines are given as a visual aid.

CONCLUSION

Unexpected T_g' vs. solution pH trends were observed for several buffers with T_g' passing through a maximum at pH 3 to 4. Such complex T_g' behavior has been explained as because of the balance between increase in viscosity due to increase in the electrostatic interactions with increasing pH, and a decrease in viscosity due to increase in amount of unfrozen water in the freeze-concentrate solution. Use of citrate buffer in freeze-dried formulations should be beneficial because of its relatively low crystallization potential and a higher collapse temperature.

ACKNOWLEDGMENTS

The study was supported by Pfizer Pharmaceutical Research and Development Summer Internship Program to Tiffany Johnson-Elton. The authors express their gratitude to Mrs. R.D. Reddy for technical assistance.

REFERENCES

1. G. Flynn. Buffers-pH Control within Pharmaceutical Systems. *J. Parenteral Drug Assoc.* **34**:139-162 (1980).
2. L. van den Berg. pH changes in buffers and foods during freezing and subsequent storage. *Cryobiology* **3**:236-242 (1966).
3. L. Van Den Berg and D. Rose. The effect of addition of sodium and potassium chloride to the reciprocal system: $\text{KH}_2\text{PO}_4\text{-Na}_2\text{HPO}_4\text{-H}_2\text{O}$ on pH and composition during freezing. *Arch. Biochim. Biophys.* **84**:305-315 (1959).
4. L. Van Den Berg and D. Rose. Effects of freezing on the pH and composition if sodium and potassium solutions: reciprocal system $\text{KH}_2\text{PO}_4\text{-Na}_2\text{HPO}_4\text{-NaH}_2\text{PO}_4\text{-H}_2\text{O}$. *Arch. Biochim. Biophys.* **81**: 319-329 (1959).

5. G. Gomez, M.J. Pikal, and N. Rodriguez-Hornedo. Effect of initial buffer composition on pH changes during far-from-equilibrium freezing of sodium phosphate buffer solutions. *Pharm. Res.* **18**:90–97 (2001).
6. T.J. Anchordoquy and J.F. Carpenter. Polymers protect lactate dehydrogenase during freeze-drying by inhibiting dissociation in the frozen state. *Arch. Biochim. Biophys.* **332**:231–238 (1996).
7. R.K. Cavatur and R. Suryanarayanan. Characterization of frozen aqueous solutions by low temperature X-ray powder diffractometry. *Pharm. Res.* **15**:194–199 (1998).
8. L. van den Berg. Changes in pH of milk during freezing and frozen storage. *J. Dairy Sci.* **14**:26–31 (1961).
9. S.S. Larsen. Studies on stability of drugs in frozen systems. VI. The effect of freezing on pH for buffered aqueous solutions. *Arch. Pharm. Chemi Sci. Ed.* **1**:41–53 (1973).
10. Y. Orii and M. Morita. Measurement of the pH of frozen buffer solutions by using pH indicators. *J. Biochem.* **81**:163–168 (1977).
12. B.S. Chang and C.S. Randall. Use of subambient thermal analysis to optimize protein lyophilization. *Cryobiology* **29**:632–656 (1992).
13. N. Murase and F. Franks. Salt precipitation during the freeze-concentration of phosphate buffer solutions. *Biophys. Chem.* **34**:293–300 (1989).
14. J.F. Carpenter, M.J. Pikal, B.S. Chang, and T.W. Randolph. Rational design of stable lyophilized protein formulations: Some practical Advice. *Pharm. Res.* **14**:969–975 (1997).
15. M.J. Akers, N. Milton, S.R. Byrn, and S.L. Nail. Glycine crystallization during freezing: the effects of salt form, pH, and ionic strength. *Pharm. Res.* **12**:1457–1461 (1995).
16. M.J. Pikal and S. Shah. The collapse temperature in freeze-drying: Dependence on measurement methodology and rate of water removal from the glassy phase. *Intern. J. Pharm.* **62**:165–186 (1990).
17. L-M. Her, M. Deras, and S.L. Nail. Electrolyte-induced changes in glass transition temperatures of freeze-concentrated solutes. *Pharm. Res.* **12**:768–772 (1995).
18. H. Levine and L. Slade. Thermomechanical properties of small carbohydrate-water glasses and “rubbers”: Kinetically metastable systems at sub-zero temperatures. *J. Chem. Soc. Faraday Trans. 1* **84**:2619–2633 (1988).
19. S.R. Aubuchon, L.C. Thomas, and H. Renner. Investigations of the sub-ambient transitions in frozen sucrose by modulated differential scanning calorimetry (MDSC). *J. Therm. Anal. Calorim.* **52**:53–64 (1998).
20. E.Y. Shalaev and F. Franks. Structural glass transition and thermophysical processes in amorphous carbohydrates and their supersaturated solutions. *J. Chem. Soc. Faraday Trans.* **91**:1511–1517 (1995).
21. Y. Roos and M. Karel. Nonequilibrium ice formation in carbohydrate solutions. *Cryo-Letters* **12**:367–376 (1991).
22. A.B. Andersen and L.H. Skibsted. Glass transition of freeze-concentrated aqueous solution of ascorbic acid as studied by alternating differential scanning calorimetry. *Lbensm.-Wiss. u.-Technol.* **31**:69–73 (1998).
23. T. Moreira. Thesis, University of Dijon, France (1976). Citation from: E. Maltini and N.M. Anese. Evaluation of viscosities of amorphous phases in partially frozen systems by WLF kinetics and glass transition temperatures. *Food Res. Int.* **28**:367–372 (1995).
24. Q. Lu and G. Zografi. Properties of citric acid at the glass transition. *J. Pharm. Sci.* **86**:1374–1378 (1997).
25. T. Osterberg and T. Wadsten. Physical state of L-histidine after freeze-drying and long-term storage. *Eur. J. Pharm. Sci.* **8**:301–308 (1999).
26. E.Y. Shalaev, F. Franks, and P. Echlin. Crystalline and amorphous phases in the ternary system water-sucrose-sodium chloride. *J. Phys. Chem.* **100**:1144–1152 (1996).
27. P. Tong and G. Zografi. Solid-state characteristics of amorphous sodium indomethacin relative to its free acid. *Pharm. Res.* **16**:1186–1192 (1999).
28. E.C. To and J.M. Flink. “Collapse”, a structural transition in freeze dried carbohydrates. II. Effect of solute composition. *J. Fd Technol.* **13**:567–581 (1978).
29. E.Y. Shalaev and F. Franks. Changes in the physical state of model mixtures during freezing and drying: impact on product quality. *Cryobiology* **33**:14–26 (1996).